LAWRENCE
LIVERMORE
NATIONAL
LABORATORY

UCRL-PROC-213217

The HCP To BCC Phase Transformation in Ti Characterized by Nanosecond Electron Microscopy

G.H. Campbell, T.B. LaGrange, W.E. King, J.D. Colvin, A. Ziegler, N.D. Browning, H. Kleinschmidt, O. Bostanjoglo

June 24, 2005

Solid-Solid Phase Transformations in Inorganic Materials 2005
Pheonix, AZ, United States
May 29, 2005 through June 3, 2005

THE HCP TO BCC PHASE TRANSFORMATION IN Ti CHARACTERIZED BY NANOSECOND ELECTRON MICROSCOPY

Geoffrey H. Campbell[1], Thomas B. LaGrange[1], Wayne E. King[1], Jeffrey D. Colvin[1], Alexander Ziegler[2], Nigel D. Browning[2], H. Kleinschmidt[3], and O. Bostanjoglo[3]

[1]University of California, Lawrence Livermore National Laboratory, Materials Science and Technology Division, 7000 East Ave., Livermore, CA 94550, USA
[2]University of California, Davis, Department of Chemical Engineering and Materials Science, One Shields Ave., Davis, CA 95616, USA
[3]Technische Universität Berlin, Optisches Institut, D-10623 Berlin, Germany

Keywords: Phase transformations, TEM, titanium

Abstract

The general class of martensitic phase transformations occurs by a rapid lattice-distortive mechanism, where kinetics and morphology of the transformation are dominated by the strain energy. Since transformation is diffusionless, phase fronts propagate through a crystal with great speed that can approach the speed of sound. We have observed a particular example of this class of phase transformation, the hexagonal close packed (HCP) to body centered cubic (BCC) transformation in titanium that is driven by a rapid increase in temperature. We have used a novel nanosecond electron microscope (the dynamic transmission electron microscope, DTEM) to acquire diffraction and imaging information on the transformation, which is driven *in-situ* by nanosecond laser irradiation. Using nanosecond exposure times that are possible in the DTEM, data can be collected about the transient events in these fast transformations. We have identified the phase transformation with diffraction patterns and correlated the time of the phase transformation with calculated conditions in the sample.

Introduction

Upon heating, Ti transforms from the HCP α phase to the BCC β phase at 1156K and melts at 1946K. This transformation is martensitic [1] and the β phase is stable over a broad temperature range, making the heating induced transformation a good candidate for observation with the DTEM. Like most rapid phase transformations, little is known of the transformation kinetics.

The DTEM is an emerging technology that combines all of the powerful techniques of the standard TEM with nanosecond time resolution for capturing dynamic processes while they occur [2-4]. Images with high spatial resolution (~1 nanometer) can be acquired that will illuminate the salient features of materials microstructure such as dislocations, impurity particles, grain boundaries, and phase boundaries. The ability to acquire multiple images during a single experiment has also been demonstrated, with frame rates exceeding 10–100 per microsecond, and higher rates within reach. This feature is particularly attractive for probing dynamic evolution in real time. Researchers at Technische Universität Berlin (TUB) [5] were the first to develop DTEM. They have applied it to several issues in the discipline of laser/materials interactions; particularly mechanisms of material removal during laser machining [6-8]. Though in its infancy, DTEM holds considerable promise as a tool for *in situ* probing for studying rapid solid-solid-phase transformations at the nanometer and nanosecond scales.

Very high time resolution is achieved by producing a short but intense burst of electrons to illuminate the specimen [9], coupled with single electron sensitive CCD image recording technology (see Figure 1 for a schematic illustration of how the DTEM functions). A

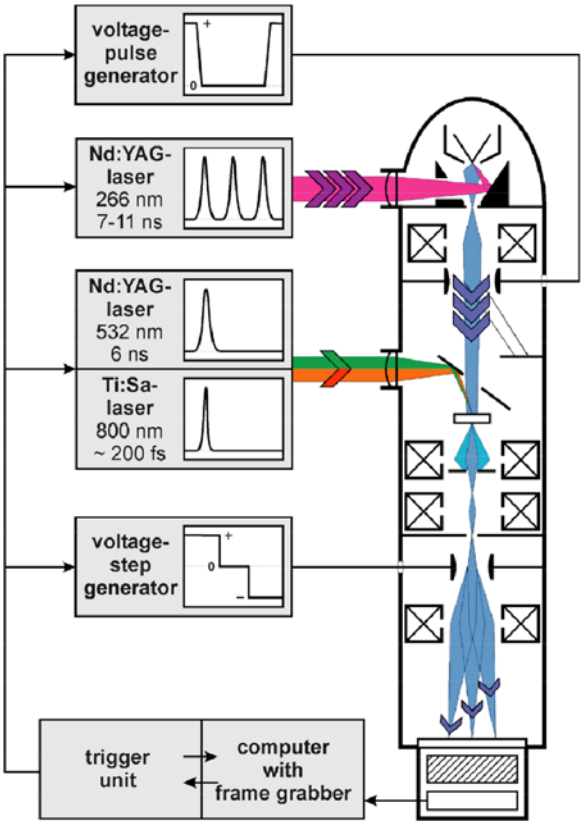

Figure 1 – Schematic illustration of the DTEM at TU Berlin that shows the cathode and treatment laser arrangements. This instrument also has multi-frame capabilities.

photocathode source (a hairpin of a low work function metal, for example zirconium) is irradiated with a pulsed UV laser with photon energy greater than the target work function. A large flux of electrons is stimulated via photoemission. The microscope processes the emitted electron "packet" in the traditional way (acceleration, focusing, magnification, detection, etc.). The sample under study is driven with a separate laser pulse. The photoemission pulse and sample pulse are synchronized to produce *in situ* measurements. It is this ability to delineate dynamic mechanisms that makes this technology particularly attractive for phase transformation studies.

Experiment

Two types of thin films (30 nm thickness) of pure Ti were created by vacuum deposition onto NaCl single crystals. The first was deposited by sputtering onto a salt crystal that was heated to 300°C. This film was highly textured with a distinct orientation relationship to the underlying salt crystal. The grain size was approximately 100 nm and each grain had one of two possible variant orientations. Each grain had $[01\bar{1}1]$ normal to the foil, while in plane one of two orientation variants, related by a 90° rotation about the foil normal, were observed (see Figure 2). The second type of thin film was made by evaporation of the Ti onto a salt substrate at room temperature. This film resulted in a very fine grain size (approximately 20 nm) with much more random orientation of the grains. Although this film produced ring patterns in the diffraction mode of the DTEM (see below) the relative intensities of the rings suggest that

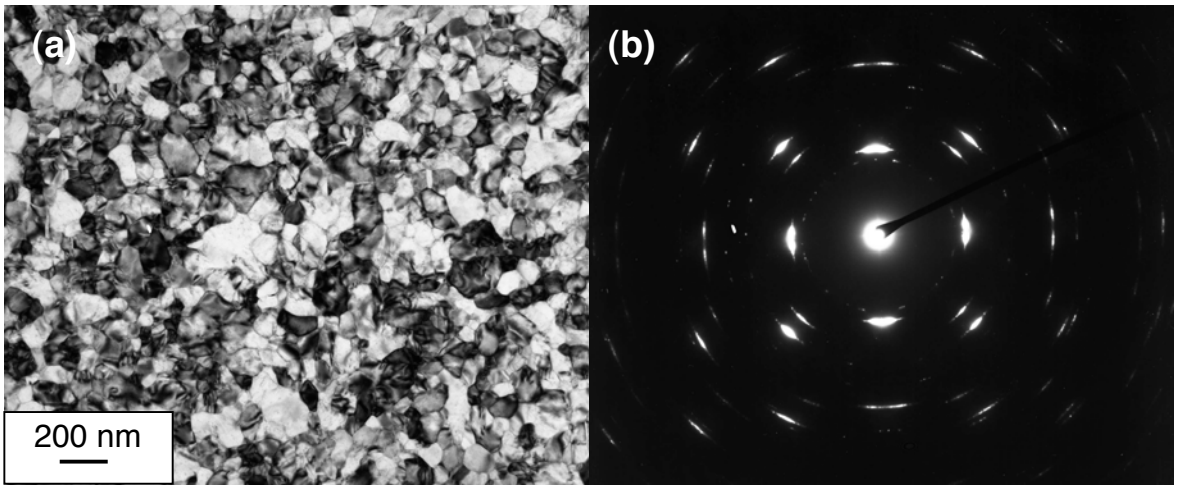

Figure 2 – (a) Standard TEM micrograph of the first type of Ti thin film produced. Although the polycrystalline nature of the foil is evident, the diffraction pattern in (b) shows a highly textured arrangement. The diffraction pattern is composed of two $[01\bar{1}1]$ patterns superimposed with a relative 90° rotation.

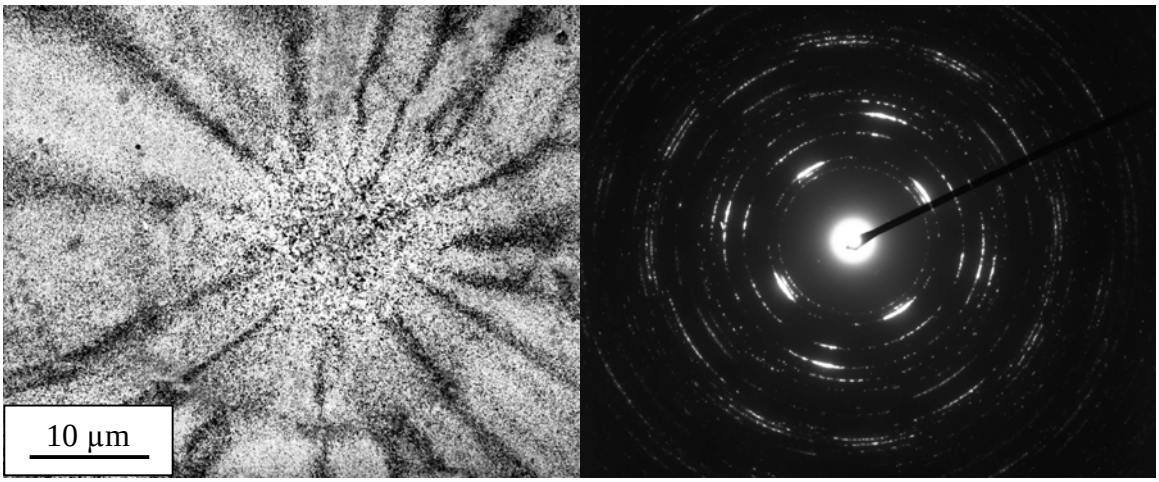

Figure 3 – Conventional TEM examination of the highly textured Ti film after treatment laser irradiation performed within the DTEM. (a) Low magnification image of the irradiated region showing central region of grain growth. (b) Selected area diffraction from the central region showing a greater extent of random crystal orientations as compared to Figure 2(b).

these films are slightly textured, where the basal planes have a slightly increased tendency to lie within the plane of the foil.

The *in-situ* experiments were performed in the DTEM by controlling the relative timing between the irradiation of the specimen with the treatment laser and the subsequent observation of the specimen with the pulse of electrons. The laser pulse energy was selected by observing when the specimen melted, evidenced by the formation of a hole [10, 11], and reducing the pulse energy until no hole was observed, which occurred at energies less than 2 μJ for the 6 ns pulse. The treatment area was a 35 μm x 60 μm (FWHM) elliptic spot on the specimen. The timing of the 7 ns electron pulse was set to range from being coincident with the treatment laser irradiation to being up to 10 μs after the treatment. The duration of this time delay could be set with an accuracy comparable to the laser pulse duration.

Results

It is instructive to first observe the effect of the treatment laser irradiation on the structure of the Ti foils. The examination of the highly textured Ti films after laser irradiation by traditional TEM is shown in Figure 3. A number of features are notable. First, at the center of laser irradiated region is seen an area having marked grain growth. Secondly, in the diffraction pattern acquired with the selected area aperture set to only sample material within this area of grain growth, the texture is significantly randomized as compared to the diffraction pattern in Figure 2b. The material outside of this central region retains the highly textured orientation exemplified by Figure 2b. Lastly, the action of the laser irradiation forms a dimple in the foil, which is shown by the symmetric array of bend contours emanating from the central region of Figure 3a.

An example of an image acquired with a 7 ns pulse of electrons on the TU Berlin

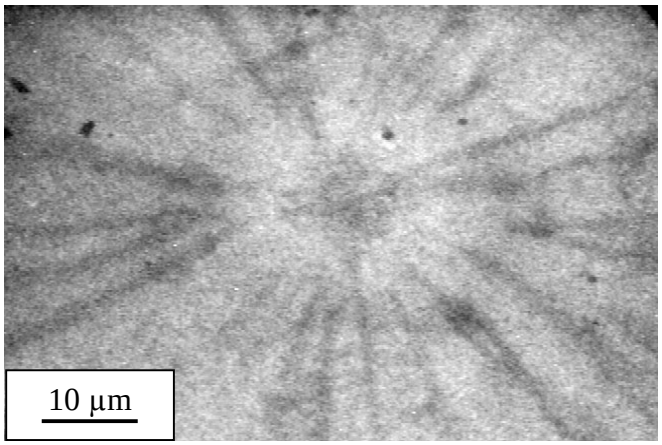

Figure 4 – An image acquired on the TU Berlin DTEM with a time resolution of 7 ns showing the region of the film irradiated by the treatment laser. The bend contours are visible due to the highly textured nature of film, producing contrast reminiscent of a single crystal.

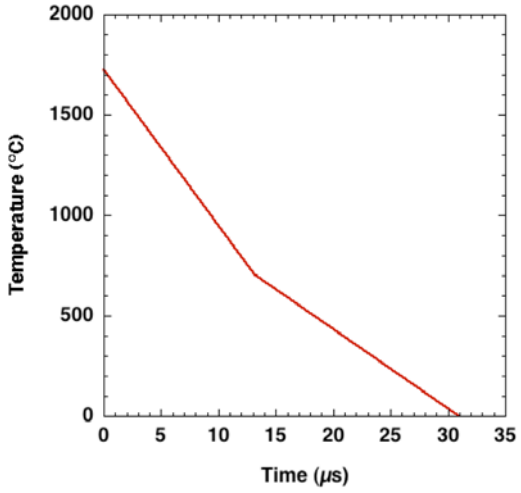

Figure 5 – A calculated time versus temperature profile for the center of the irradiated region.

DTEM is shown in Figure 4. Like Figure 3, this image is of a laser-irradiated area some minutes after the actual irradiation. The bend contours are clearly evident, indicating that the electron pulse has sufficient coherence to retain the dynamical diffraction character that is essential for high-resolution image formation in the TEM. However, as is especially noticeable in the central region of the image, the large grains are not imaged. This degradation in image resolution is due to noise from the limited number of electrons in the pulse (approximately 5×10^7 e^-) and from the image amplification system in the detector.

Figure 5 shows a calculated temperature versus time profile for the Ti films at the center of the treatment laser irradiation area. This curve was calculated by considering the energy deposited in the foil by the laser pulse, the heat capacity, and the thermal diffusivity within the foil. Radiative dissipation of the energy was found to be negligible. The sample is heated during the initial 7 ns, which is too short to resolve in the plot, and then cools to room temperature within 30 μs. All the microstructural evolution observed in Figure 3 occurs during this short time.

Due to the limited resolution of the DTEM images, it was difficult to obtain useful information from images about the microstructural changes occurring in the Ti films during transformation. With the second type of thin foil, the random crystallographic orientation of the grains prevented any contrast from appearing, as opposed to what can be seen in Figure 4. However, the diffraction patterns were useful for determining the phase present in the sample as a function of time. Examples of the diffraction patterns are shown in Figure 6. Since these patterns are acquired in a single shot mode, a new area of the specimen was chosen for each experiment. The time delay between the treatment laser irradiation and acquisition of a diffraction pattern was varied. The diffraction patterns were rotationally summed and the results are shown in Figure 7. To investigate microstructural evolution while the specimen is in the BCC phase the relative intensities of the diffraction rings was quantified. The background of the curves shown in Figure 7 was fit with a 2nd order polynomial, and the peaks were fit with Lorentzian curves. An example of the fit is shown in Figure 8. Finally, the areas of the fit Lorentzian curves were used to determine the ratios of peak intensities plotted in Figure 9.

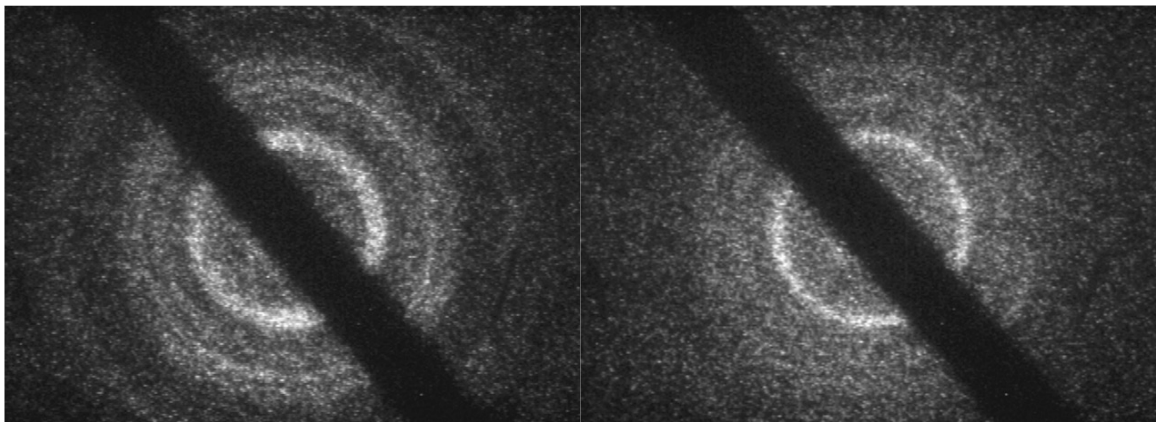

Figure 6 – Diffraction patterns recorded with 7 ns time resolution of the fine-grained, more randomly textured foils. The ring patterns are identified as arising from (a) the hcp crystal structure and (b) the bcc crystal structure. The pattern in (a) was acquired at room temperature. The pattern in (b) was acquired at 2.5 μs after treatment laser irradiation.

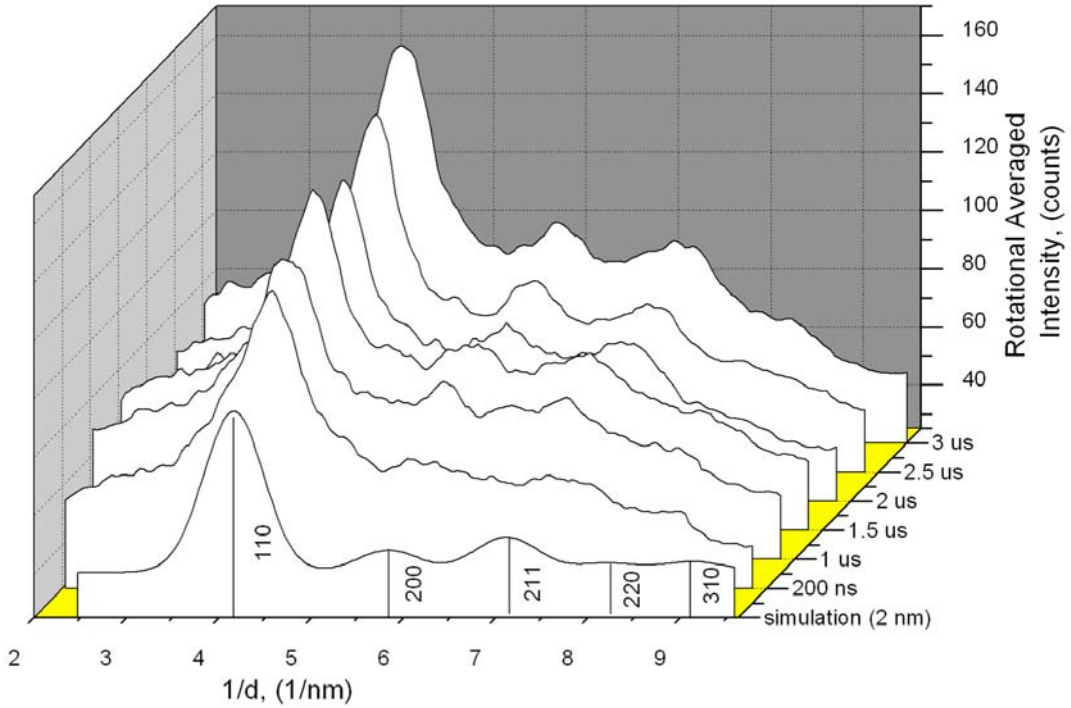

Figure 7 – The rotationally averaged diffraction intensities as a function of time delay after treatment laser irradiation. The first curve is a simulation based on a random texture. A slight amount of texture is observed in the experimental curves. The diffraction signal improves as a function of time due to the specimen cooling (see Fig. 5), reducing thermal scattering effects.

Discussion

The *ex-situ* examination of the laser irradiated foils revealed grain growth and texture randomization within the central area of the laser spot, as seen in Figures 2 and 3. These processes take place during the limited time that the foil experiences elevated temperatures. The duration of these high temperatures is less than 30 μs (Figure 5). The randomization of the texture is likely assisted by the phase transformation from the high temperature BCC to the low temperature HCP phase. Nucleation of the HCP seems to occur, in at least some of the grains, with random orientations.

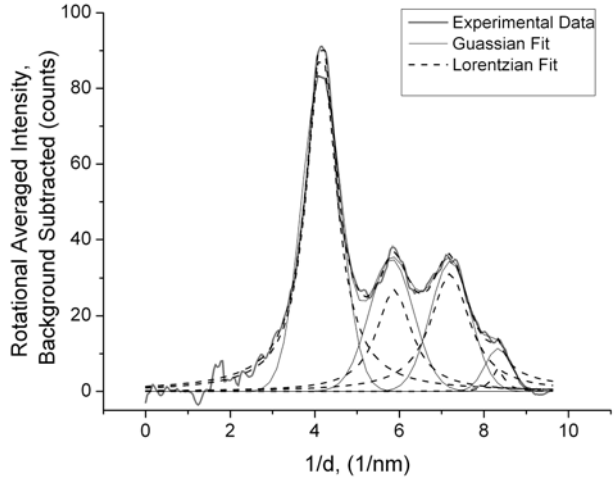

Figure 8 – Example of the peak fit used to quantify relative diffraction peak intensities. Lorentzian and Guassian curves are compared, showing the improvement for the Lorentzian fit.

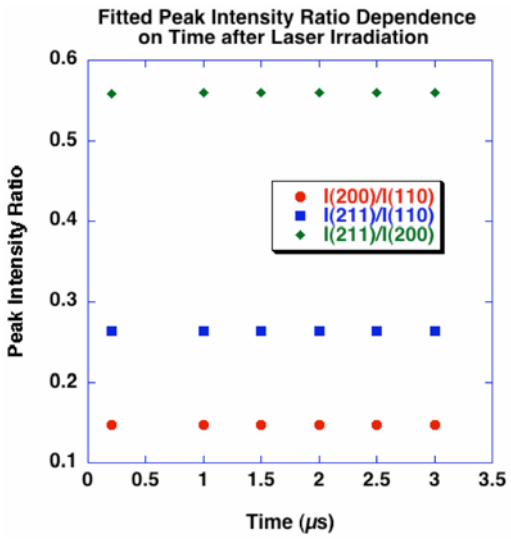

Figure 9 – The relative peak intensity ratios plotted as a function of time past the treatment laser irradiation time.

This behavior is contrasted with the *in-situ* observations of the BCC phase while it exists for the short period of time during which the foil is at high temperature. For the 3 μs after laser irradiation, the relative diffracted peak intensities do not change, indicating that the texture does not change. This observation reaffirms the notion that the renucleation of the HCP phase on cooling creates the texture randomization observed in the *ex-situ* characterization. The reversion to HCP was observed to occur at about 6 μs after the treatment laser irradiation, in rough agreement with the calculated temperature-time profile in Figure 5.

Conclusions

The technique of DTEM has proven useful for the *in-situ* observation of fast, solid-solid phase transformations in materials. We have observed the Ti BCC phase *in-situ* with diffraction patterns while it exits after transient heating by a 6 ns laser pulse. The BCC phase reverts to the HCP phase after cooling over a time span of 6 μs, in agreement with a calculated temperature profile dominated by heat transfer by conduction within the Ti foil. For times shorter than approximately 200 ns after treatment laser irradiation, thermal scattering effects made the interpretation of the diffraction patterns ambiguous. The cooling of the sample for all times after 200 ns made the signal to background ratio of the diffraction patterns continuously improve.

Acknowledgements

This work performed under the auspices of the U. S. Department of Energy by the University of California, Lawrence Livermore National Laboratory under Contract No. W-7405-Eng-48.

References

1. W. Zhang, W. S. Zhao, D. X. Li and M. L. Sui, "Martensitic transformation from α-Ti to β-Ti on rapid heating," *Applied Physics Letters*, 84 (24) (2004), 4872 - 4874.
2. O. Bostanjoglo, "High - speed electron microscopy," *Advances in imaging and electron physics*, 121 (2002), 1 - 51.
3. O. Bostanjoglo, R. Elschner, Z. Mao, T. Nink and M. Weingärtner, "Nanosecond electron microscopes," *Ultramicroscopy*, 81 (3 - 4) (2000), 141 - 147.
4. H. Dömer and O. Bostanjoglo, "High-speed transmission electron microscope," *Reviews of Scientific Instruments*, 74 (10) (2003), 4369 - 4372.
5. O. Bostanjoglo and R. Liedtke, "Tracing Fast Phase Transformations by Electron Microscopy," *Physica Status Solidi A*, 60 (2) (1980), 451 - 455.
6. H. Dömer and O. Bostanjoglo, "Laser ablation of thin films with very high induced stresses," *Journal of Applied Physics*, 91 (8) (2002), 5462 - 5467.
7. H. Dömer and O. Bostanjoglo, "Stress effects in laser-pulsed chromium films tracked by nanosecond transmission electron microscopy," *Advanced Engineering Materials*, 4 (8) (2002), 623 - 625.
8. H. Dömer and O. Bostanjoglo, "Phase explosion in laser-pulsed metal films," *Applied Surface Science*, 208 - 209 (2003), 442 - 446.
9. B. Schafer and O. Bostanjoglo, "Laser Driven Thermionic Electron Gun," *Optik*, 92 (1) (1992), 9-13.
10. T. Nink, G. F., Z. L. Mao and O. Bostanjoglo, "Dynamics of laser pulse-induced melts in Ni-P visualized by high-speed transmission electron microscopy," *Applied Surface Science*, 139 (1999), 439 - 443.
11. T. Nink, Z. L. Mao and O. Bostanjoglo, "Melt instability and crystallization in thin amorphous Ni-P films," *Applied Surface Science*, 154 (2000), 140 - 145.